Tunable diffractor using liquid crystals and carbon black nanoparticles

ChaeLim Han[a], Yeon Jin Han[b], GyuRi Choi[b], Young Jin Lim[a], Seung Hee Lee[a,b,c*] and MinSu Kim[b*]
[a]Dept. of JBNU-KIST Industry-Academic Convergence Research, Jeonbuk National University, Jeonju, Jeonbuk 54896, Korea; [b]Dept. of Nano Convergence Engineering, Jeonbuk National University, Jeonju, Jeonbuk 54896, Korea; [c]Dept. of Polymer Nano Science and Technology, Jeonbuk National University, Jeonju, Jeonbuk 54896, Korea

ABSTRACT

We investigate two tunable transmission diffractors: utilizing nano droplet polymer-dispersed liquid crystals (nano-PDLCs) and electrophoretic carbon black (CB) nanoparticles. Both approaches use similar electric field formation using interdigitated electrodes while the nano-PDLC utilizes electric field-induced phase modulation (induced birefringence) by Kerr effect from an optically isotropic transparent state and the CB diffractor generates slit and switches the slit distance in between dark region. The CB diffractor is polarization independent on an incident light and so is its diffracted beam whereas the nano-PDLC diffractor is polarization dependent. The CB diffractor can tune the diffraction slit width and angle by controlling the applied voltage. The complementary properties of nano-PDLC and CB nanoparticles offer applications for various optical modulation needs.

Keywords: tunable diffractors, carbon black nanoparticles, optically isotropic nano-droplet liquid crystals

1. INTRODUCTION

When light propagates and encounters an object, its waves may scatter and interfere constructively or destructively. Periodic apertures can significantly enhance light diffraction, a phenomenon widely utilized in applications such as data storage technologies, X-ray crystallography, monochromators, spectrometers, and wavelength division multiplexing devices [1]. Recent advancements in this field focus on developing tunable diffractors, which allow for the dynamic modification of aperture periodicity within a single device.

In this study, we present a tunable diffractor based on carbon black (CB) nanoparticles, compared with one using nano polymer-dispersed liquid crystals (nano-PDLCs). Both systems can adjust their diffraction patterns and angles [2,3]. The nano-PDLC diffractor relies on phase modulation induced by the Kerr effect, which occurs periodically on a patterned interdigitated electrode. In contrast, the CB diffractor employs electrophoresis, where CB particles aggregate along the electrode structure to form periodic slits. By applying electric fields, the periodicity and corresponding diffraction angle can be dynamically tuned.

The CB-based diffractor offers several advantages, including polarization-independent diffraction and an operational temperature range exceeding 170°C, which is approximately 70°C broader than that of the nano-PDLC diffractor. Depending on environmental conditions and the need for polarization-independent operation, CB diffractors can provide unique benefits, while nano-PDLC diffractors are more suitable for applications requiring different performance characteristics.

2. EXPERIMENTAL

Cell Structures

Both devices are fabricated with indium-tin-oxide (ITO) coated plain and interdigitated electrodes. The interdigitated electrodes of the nano-PDLC have a width *w*, distance between electrodes *l*, and cell gap *d* of 4 μm. In the CB diffractor,

Emerging Liquid Crystal Technologies XX, edited by Liang-Chy Chien, Nelson V. Tabiryan, Jun Yamamoto, Proc. of SPIE Vol. 13387, 133870F · © 2025
SPIE · 0277-786X · doi: 10.1117/12.3041169

w =7 µm, l =15 µm, and d =11 µm, and additionally an organic insulating layer is coated on both electrode surfaces to prevent electrical shorts.

Mixtures

Nano-PDLC mixture consists of a high dielectric nematic LC (MLC-2053), polymer (NOA65), and photo-initiator (Irgacure 907). For CB diffractor, the CB nanoparticles (average size: 98 nm) are uniformly dispersed in dielectric media (Isopar M and Halocarbon oil 0.8).

Driving Methods

The nano-PDLC has two driving modes: in-plane fields (IPS) mode, vertical-in-plane fields (VIS) mode. In IPS mode, lateral electric field is applied between branches of bottom interdigitated electrodes. In VIS mode, a constant offset voltage ($V_{offset} \neq 0$) is applied to the top plain electrode while maintaining the IPS electric field at the bottom, resulting in the formation of both vertical and horizontal electric fields [2]. In CB diffractors, the uniformly dispersed, negatively charged CB nanoparticles move to the positively charged electrodes to form dark periodic slits. Positive voltages are applied to one branch (wide-slit mode) or both branches (narrow-slit mode) of the interdigitated electrodes to switch the slit periodicity as well as diffraction angle.

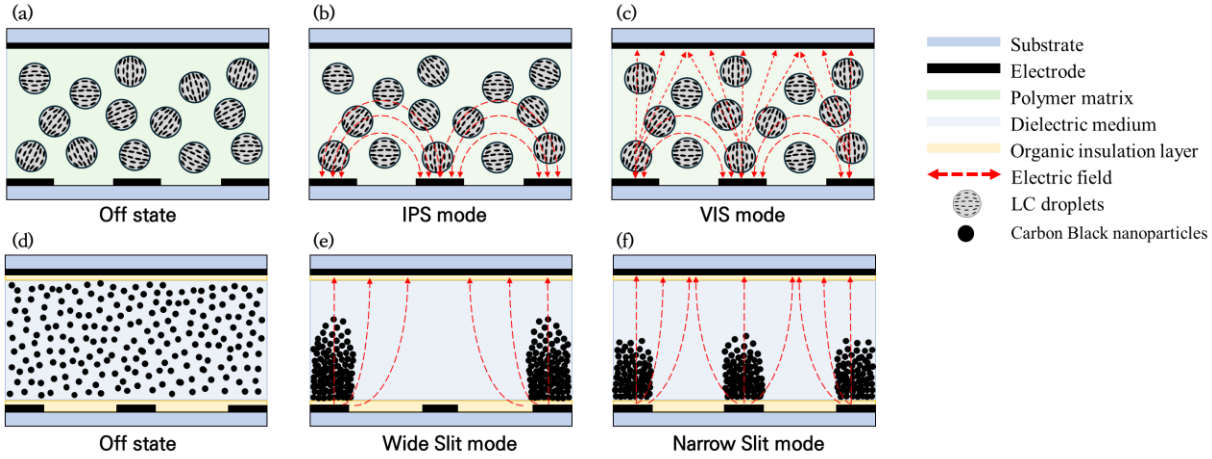

Figure 1. Driving schemes of nano-PDLC and CB diffractor. *(a-c)* nano-PDLC and *(d-f)* CB diffractor. *(a)* nano-PDLC initially has a randomly oriented dropelet of LCs. There are two switching modes, *(b)* IPS mode, *(c)* VIS mode. *(d)* CB particles well dispersed with no voltage. CB particles aggregate at the electrodes with (+) voltage applied at *(e)* wide-slit mode and *(f)* narrow-slit mode.

3. RESULTS AND DISCUSSION

Diffraction patterns, OM images and diffraction angles

In Figure 2, the nano-PDLC was driven by V_{ac} = 50 V in the IPS mode, and V_{ac} = 50 V, and V_{offset} = 20 V in the VIS mode. (w = 4 µm, l = 4 µm, d = 4 µm). The diffraction pattern was captured as optical setup with the light source (He-Ne laser, λ = 632.8 nm), polarizer, sample, and black screen in order, and the distance between the sample and screen was 72 cm.

According to Figure 2, the diffraction pattern of nano-PDLC changes from the initial state *(a)* with no applied voltage to *(b)* and *(c)* in IPS and VIS modes. In the VIS mode, additional LC reorientation to the IPS mode exists in the region responding to vertical electric fields and contributes to higher spatial phase difference.

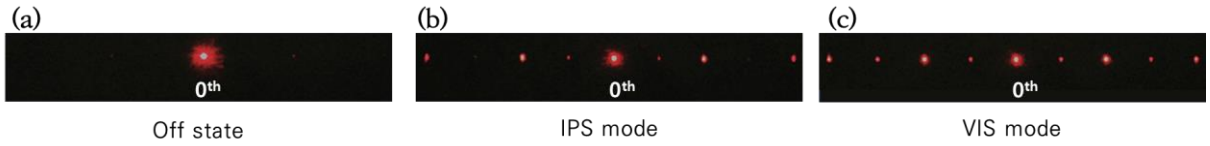

Figure 2. Diffraction patterns of nano-PDLC when *(a)* initial state with no voltage; when applying voltage in *(b)* IPS mode, and *(c)* VIS mode.

Diffraction patterns and optical microscopy images of CB nanoparticle diffractor, driven at 0.81 V/μm in wide-slit mode (Figure 3(*b, e*)) and 1.27 V/μm in narrow-slit mode (Figure 3(*e, f*)), were obtained using the same optical setup as in Figure 2 except for no polarizer and the distance of 33 cm between the sample and screen. When applying voltage to one branch of the interdigitated electrode, the slit distance becomes broader in the wide-slit mode as shown in Figure 3*(e)*. By applying voltage to both branches in the narrow-slit mode as shown in Figure 3*(f)*, the number of slits becomes doubled.

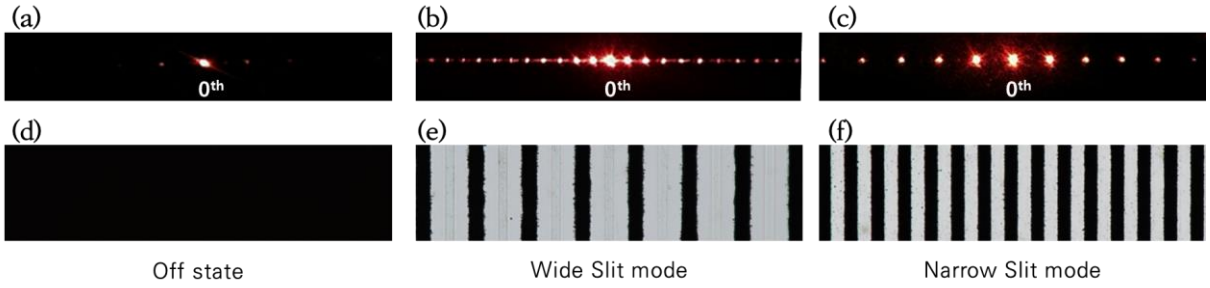

Figure 3. *(a-c)* Diffraction patterns and *(d-f)* optical microscope images of CB diffractor. *(a, d)* The diffraction states with (*d*) no voltage and applying voltage in the *(b, e)* wide-slit mode and *(c, f)* narrow- slit mode. The optical microscope images were taken at 200x magnification.

To verify the diffraction angle difference by the slit distance changes we checked the experimental measurement with theoretically calculated diffraction angles based on equation (1) and (2) as below.

$$tan\,\theta_m = \frac{D_m}{L} \qquad (1)$$

where D_m is the separation between m_{th} and zeroth order, L is the distance between the diffractor and the screen. The distance between the diffracted beams and the zeroth order beam was measured, and the experimental diffraction angle was obtained using the equation (1).

The theoretical diffraction angle was obtained as below,

$$\sin\theta_m = \frac{m\lambda}{\Lambda} \qquad (2)$$

where Λ is $(w + l)$ the pitch of the grating, and m is the diffraction order $(0, \pm 1, \pm 2, \pm 3, \cdots)$.

The measured and calculated results are organized in Table 1, which shows the diffraction pattern distance and diffraction angle for different driving methods. Based on the result, we verified that as the slit distance is narrowed down, the diffraction angle gets wider.

Diffraction order	**IPS** mode in nano-PLDC			**VIS** mode in nano-PDLC		
	$\boldsymbol{D_m}$ (cm)	$\boldsymbol{\theta_m}$ (º) (experimental)	$\boldsymbol{\theta_m}$ (º) (theoretical)	$\boldsymbol{D_m}$ (cm)	$\boldsymbol{\theta_m}$ (º) (experimental)	$\boldsymbol{\theta_m}$ (º) (theoretical)

1st	6.9	5.47	5.57	6.9	5.47	5.57
2nd	14	11.0	11.19	14	11.0	11.19

Diffraction order	**Wide-slit** mode in CB diffractor			**Narrow-slit** mode in CB diffractor		
	D_m (cm)	θ_m (º) (experimental)	θ_m (º) (theoretical)	D_m (cm)	θ_m (º) (experimental)	θ_m (º) (theoretical)
1st	0.4	0.7	0.8	0.9	1.6	1.7
2nd	0.8	1.4	1.7	1.8	3.1	3.3

Table 1. The measured and calculated values of diffraction depending on the driving method of nano-PDLC and CB diffractor.

Diffraction efficiency depending on driving mode

The diffraction efficiency of the device was determined using a photodetector in front of the screen in the same setup as when capturing the diffraction pattern images. The diffraction efficiency was then calculated as,

$$\eta_m(\%) = \frac{I_m(V)}{I_0} \times 100 \qquad (3)$$

where $I_m(V)$ is intensity of m_{th} order subjected to voltage V, and I_0 is total intensity of incident light at the field-off state.

The nano-PDLC shows higher diffraction efficiency in the VIS mode than IPS mode due to the added vertical electric field between top and bottom electrodes. Based on the measured values of each nano-PDLC and CB diffractor, we also found that the CB diffractor shows higher diffraction efficiency in the narrow-slit mode than in the wider-slit mode as shown in Figure 4.

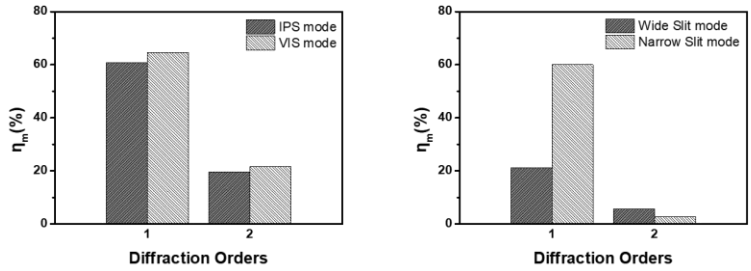

Figure 4. Diffraction efficiency of (*a*) the nano-PDLC and (*b*) CB nanoparticle diffractors, depending on driving method.

Polarization dependency

To verify the polarization dependency, we measured the intensity of the 1st order diffracted beam after we added an analyzer in between the sample and photodetector, and the analyzer was fixed while the polarizer was rotated. With or without cell placed, the angle-dependent intensity curves of the 1st order diffraction are in similar trend, which proves the polarization independency of the CB diffractor.

Based on the Kerr effect, the electric field application induces birefringence in the nano-PDLC while CB nanoparticles are isotropic. The electric field formation gives rise to difference LC reorientation direction, which gives periodic phase difference along the electrodes. The diffraction efficiency depends on the regional polarization modulation as the maximum diffracted intensity occurs when the phase difference gets significant. On the contrary, the CB diffractors absorb light and

allow light diffracted along the slits. Thus, the diffraction efficiency of CB diffractor is independent on the polarization as shown in Figure 5.

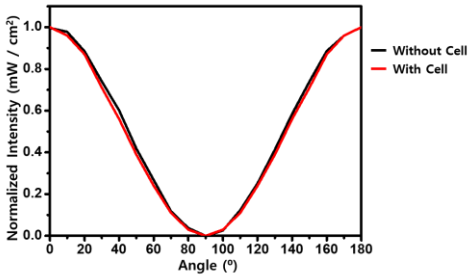

Figure 5. Verification of polarization dependency in CB diffractor.

Temperature dependency

The optical microscope images and diffraction patterns were taken on a hot stage to control the temperature for verifying the temperature dependency. The LCs have a nematic-isotropic and nematic-crystal phase transition temperature (T_{NI} = 86℃ and T_{NC} = -10℃) for MLC-2053, so that nano-PDLC can only operate in the range between T_{NC} and T_{NI}. The CB nanoparticles are thermally more stable than LCs. As shown in Figure 6, the diffraction pattern was stable when changing temperature from -50°C to 100°C; almost no change from 23°C was observed.

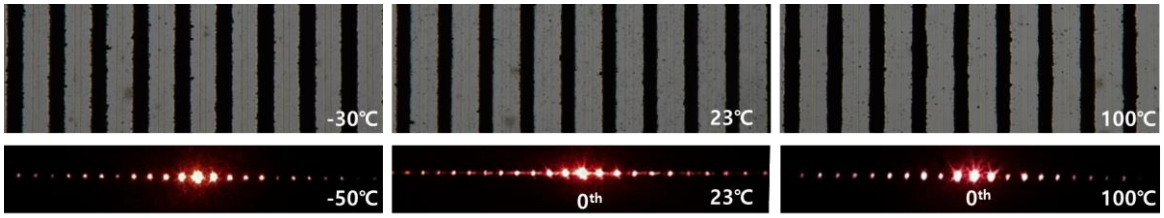

Figure 6. Optical microscopy images and diffraction patterns of CB diffractor at different temperatures.

4. CONCLUSIONS

In this study, we demonstrated and compared the electro-optical and thermal properties of both nano-PDLC and CB nanoparticle diffractors. Both systems can adjust their diffraction patterns and angles depending on the driving mode, with the diffraction angle further influenced by the dimensions of the patterned electrodes. The CB diffractor, in particular, offers polarization independence and a wide operating temperature range. This comparison highlights the distinct advantages of each system, making them suitable for different application environments and conditions.

ACKNOWLEDGEMENTS

This work was supported by the Commercialization Promotion Agency for R&D Outcomes (COMPA) grant funded by the Ministry of Science and ICT [RS-2023-00304743].

REFERENCES

[1] T. K. Gaylord and M. G. Moharam, “Analysis and applications of optical diffraction by gratings,” 73, Proceedings of the IEEE, 894-937 (1985); https://doi.org/10.1109/PROC.1985.13220

[2] Pagidi, S., Kim, M.S., Manda, R., Ahn, S., Jeon, M. Y., & Lee, S. H., "Ideal micro-lenticular lens based on phase modulation of optically isotropic liquid crystal-polymer composite with three terminals," Journal of Molecular Liquids, 380, 121730 (2023); https://doi.org/10.1016/j.molliq.2023.121730
[3] Lim, Y. J., Jeon, H. S., Han, Y. J., Kim, T. H., Kim, M.S., & Lee, S. H., "Haze-Suppressed Wideband Light Shutter from Near Ultraviolet to Infrared Rays Utilizing Electrophoretic Carbon Black Particles," Small, 20(3), 2305531 (2024); https://doi.org/10.1002/smll.202305531